Applied Radiation and Isotopes 162 (2020) 109179

Contents lists available at ScienceDirect

Applied Radiation and Isotopes

journal homepage: http://www.elsevier.com/locate/apradiso

A revision of the virtual point detector model for calculating NaI(Tl) detector efficiency

Huynh Dinh Chuong [a,c], Le Thi Ngoc Trang [a,c], Vo Hoang Nguyen [b,c], Tran Thien Thanh [a,b,c,*]

[a] Nuclear Technique Laboratory, University of Science, Ho Chi Minh City, Viet Nam
[b] Department of Nuclear Physics, Physics and Engineering Physics, University of Science, Ho Chi Minh City, Viet Nam
[c] Vietnam National University, Ho Chi Minh City, Viet Nam

ARTICLE INFO

Keywords:
Virtual point detector
NaI(Tl) detector
Full energy peak efficiency

ABSTRACT

In present work, the validity of the virtual point detector (VPD) model for the NaI(Tl) detectors is studied and confirmed in the photon energy range of 60–1408 keV. The full energy peak efficiency (FEPE) of two NaI(Tl) detectors, which have scintillation crystal dimensions of 5.08 × 5.08 cm and 7.62 × 7.62 cm respectively, is measured for "point-like" radioactive sources on the symmetry axis with source-to-detector distances in the range of 2–40 cm. It is found that the VPD model is valid to fit too well to the experimental FEPE for the two surveyed NaI(Tl) detectors. The dependence of the VPD position on the incident photon energy for the NaI(Tl) detectors with different scintillation crystal dimensions is shown based on experimental data. A semi-empirical equation involving incident photon energy and source-to-detector distance is proposed to calculate the FEPE for the NaI (Tl) detectors. The calculated results for the two surveyed NaI(Tl) detectors by this equation are in a good agreement with experimental results for photon energies in the range of 344–1408 keV. However, the difference between experimental and calculated results is quite significant for source-to-detector close geometries for photon energies lower than 344 keV.

1. Introduction

An accurate knowledge of the FEPE is required for the operation of gamma-ray spectrometry applications in numerous fields, such as measurements of the absolute activity of gamma emitting radionuclides and calculation of the absorbed doses. The FEPE varies strongly with the source-to-detector distance and incident photon energy, due to the geometry and absorption factors. Thus, the calibration of FEPE for each measuring configuration is necessary. It is useful to study a mathematical model for quick and simple calculation of the FEPE at any source-to-detector distance with satisfactory accuracy. However, the dependence of FEPE on source-to-detector distance is generally a complex function of the shape, dimensions of detector and measurement geometry. This causes difficulty in calculating the effect of the varying distances. The VPD model was introduced by Notea (1971) for Ge(Li) detector to deal with this problem. It is suggested that the detector volume may be replaced for the FEPE calculations by a virtual equivalent point detector on the symmetry axis of the detector. Based on this model, the FEPE of the detector is represented by a simple quadratic inverse function of the source-to-VPD distance. Therefore, the VPD model can be used for facilitating FEPE calculations. Later, the VPD model was widely investigated for the HPGe detectors (Hoover, 2007; Mahling et al., 2006; Mohammadi et al., 2011; Presler et al., 2006).

The NaI(Tl) detectors are one of the most commonly used instruments for gamma-ray spectrometry applications in experimental nuclear physics. It is necessary to evaluate the accuracy and reliability of the FEPE calculations for NaI(Tl) detectors by the VPD model. In the past, the interpolation and extrapolation of counting efficiency of NaI (Tl) and BGO scintillation detectors for measurements of "point-like" radioactive sources (Presler et al., 2006) based on VPD model were investigated. However, in this report, the authors concluded that the VPD model does not seem to fit too well to the experimental data for the whole range (from 1 to 18 cm) of source-to-detector distances; VPD positions are constant and independent of incident photon energy. The calculated efficiencies show a quite high discrepancy from the measured efficiencies for photon energies in the range of 238–2614 keV, with the relative deviations up to several tens in percents. So, the question is whether the VPD model is really not suitable for the NaI(Tl) scintillation

* Corresponding author. Department of Nuclear Physics, Faculty of Physics and Engineering Physics, University of Science, VNU-HCM, 227, Nguyen Van Cu Street District 5, Ho Chi Minh City, Viet Nam.
E-mail address: ttthanh@hcmus.edu.vn (T.T. Thanh).

https://doi.org/10.1016/j.apradiso.2020.109179
Received 14 October 2019; Received in revised form 27 February 2020; Accepted 6 April 2020
Available online 10 April 2020

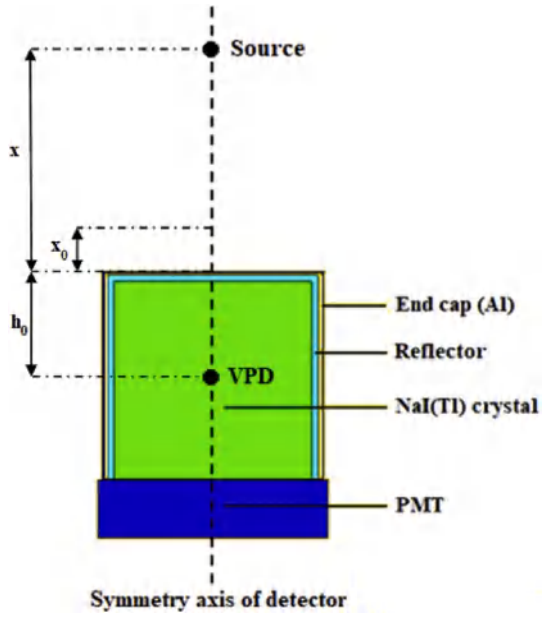

Fig. 1. Schematic representation of VPD model for NaI(Tl) detector and a point radioactive source on symmetry axis of detector.

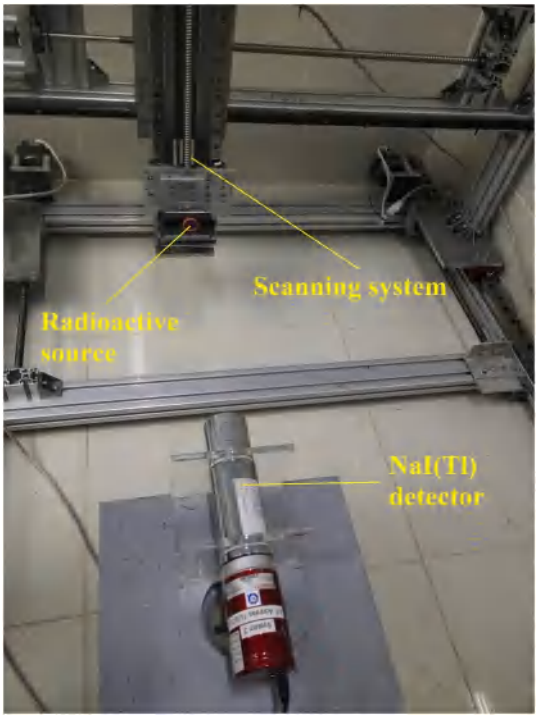

Fig. 2. Picture of the experimental set-up.

detectors. Besides, there is still a lack of experimental data to show the dependence of the VPD position on the incident photon energy and the NaI(Tl) crystal dimensions, although simulation study have been reported by Rubin et al. (2019).

This paper provides a revision of the validity of the VPD model for calculating the FEPE of NaI(Tl) detectors. Measurements of "point-like" radioactive sources on the symmetry axis at several source-to-detector distances for two NaI(Tl) detectors, with scintillation crystal dimensions of 5.08 × 5.08 cm and 7.62 × 7.62 cm, are performed to obtain the FEPE in the photon energy range of 60–1408 keV. The validity of the VPD model for NaI(Tl) detectors is confirmed based on experimental

Table 1
Summarization of the relevant data for radioactive sources used in this study.

Source	Half-life	Energy (keV)	Photon emission probability (%)	Activity (kBq)
^{22}Na	2.6029 (8) years	511	180.7 (2)	8.5 (3)
		1275	99.94 (13)	
^{60}Co	5.2711 (8) years	1173	99.85 (3)	20.8 (6)
		1333	99.9826 (6)	
^{137}Cs	30.05 (8) years	662	84.99 (20)	34 (1)
^{152}Eu	13.522 (16) years	122	28.41 (13)	235 (7)
		245	7.55 (4)	
		344	26.59 (12)	
		779	12.97 (6)	
		964	14.50 (6)	
		1408	20.85 (8)	
^{241}Am	432.6 (6) years	60	35.92 (17)	34 (1)

Note: 8.5 (3) = 8.5 ± 0.3. The values of half-life, energy and photon emission probability for the radionuclides in Table 1 are used from recommended data of Laboratoire National Henri Becquerel (Laboratoire National Henri Becquerel, 2019).

FEPE at several source-to-detector distances in the range of 2–40 cm. The dependence of the VPD position on the incident photon energy for the NaI(Tl) detectors with different scintillation crystal dimensions is shown based on experimental data. Then, a semi-empirical equation involving incident photon energy and source-to-detector distance is proposed to calculate the FEPE for the two surveyed NaI(Tl) detectors. The reliability of this semi-empirical equation is evaluated by comparing the calculated and experimental results.

2. Methodology

The schematic representation of VPD model for NaI(Tl) detector and a point radioactive source on symmetry axis of detector is shown in Fig. 1. In here, the detector volume is replaced by a VPD on the symmetry axis of detector at distance h_0 from the end cap. The distance of the point radioactive source from the end cap of detector is denoted by x. Based on the VPD model, the FEPE of detector for measurements of a point radioactive source in non-absorbing media only obeys the quadratic inverse law of the source-to-VPD distance ($x + h_0$). Thus, the ratio of the FEPE for two source-to-detector distances (x_0 and x) can be represented by the following equation [2]:

$$\frac{\varepsilon(x_0)}{\varepsilon(x)} = \frac{(x+h_0)^2}{(x_0+h_0)^2} \quad (1)$$

where $\varepsilon(x_0)$ and $\varepsilon(x)$ are the FEPE of detector corresponding to the source-to-detector distances x_0 and x, respectively.

Rearranging Eq. (1) yields:

$$\sqrt{\frac{\varepsilon(x_0)}{\varepsilon(x)}} - 1 = \frac{1}{(x_0+h_0)}(x - x_0) \quad (2)$$

The validity of the VPD model for NaI(Tl) detectors can be verified based on Eq. (2). Specifically, x_0 is treated as a constant reference distance and x is a variable distance. Then, the experimental values of $\sqrt{\varepsilon(x_0)/\varepsilon(x)} - 1$ versus $(x - x_0)$ are fitted by the least-squares method with a linear function. If the VPD model is indeed valid for an investigated detector, the values of the correlation coefficient R^2 (adjusted R-squared) and the intercept coefficient of fitting functions must be approximately 1 and 0, respectively. Besides, the position of VPD on the symmetry axis of the detector (h_0) can be determined from the slope coefficient of fitting functions. The uncertainty of h_0 is calculated by the propagation error formula with the uncertainty components of the position of point source and the slope coefficient of fitting function. It

Table 2
Coincidence summing correction factors of ^{22}Na,^{60}Co,^{152}Eu sources for several source-to-detector distances for two surveyed NaI(Tl) detectors.

	Coincidence summing correction factor								
E (keV)	511	1275	1173	1333	122	344	779	964	1408
x (cm)									
NaI(Tl) 5.08×5.08 cm detector (Detector A)									
2	1.053	1.151	1.054	1.058	1.195	1.051	1.087	1.236	1.237
5	1.019	1.050	1.020	1.021	1.060	1.019	1.027	1.066	1.070
8	1.010	1.024	1.011	1.011	1.028	1.009	1.014	1.029	1.031
10	1.007	1.016	1.007	1.008	1.019	1.007	1.010	1.018	1.021
12	1.005	1.012	1.005	1.006	1.013	1.005	1.006	1.013	1.014
15	1.003	1.007	1.004	1.004	1.009	1.004	1.004	1.009	1.009
18	1.003	1.005	1.003	1.003	1.006	1.002	1.003	1.006	1.006
NaI(Tl) 7.62 × 7.62 cm detector (Detector B)									
2	1.110	1.323	1.113	1.118	1.355	1.101	1.168	1.408	1.388
4	1.057	1.151	1.060	1.063	1.174	1.052	1.081	1.191	1.190
6	1.035	1.088	1.037	1.038	1.100	1.032	1.047	1.106	1.107
8	1.023	1.057	1.025	1.026	1.064	1.021	1.030	1.065	1.068
10	1.017	1.040	1.018	1.019	1.044	1.016	1.020	1.044	1.046
12	1.013	1.030	1.013	1.014	1.033	1.011	1.015	1.032	1.032
14	1.010	1.023	1.010	1.011	1.025	1.009	1.011	1.023	1.024
16	1.008	1.018	1.009	1.009	1.019	1.008	1.010	1.018	1.019
18	1.007	1.014	1.007	1.007	1.016	1.006	1.007	1.014	1.015

should be stressed that the VPD has no physical meaning but only a mathematical model to simply describe the relationship between the FEPE and source-to-detector distance. However, the position of the VPD reflects the characteristics of the measurement. Obviously, for a specific source-to-detector distance, the FEPE depends on the incident photon energy and the scintillation crystal dimensions. Therefore, it is expected that the VPD position will be affected by these factors. Besides, the selection of the reference distance x_0 can also affect the VPD position. These issues need to be evaluated in detail by experimental data.

Assume that h_0 can be expressed as a function of the incident photon energy for each NaI(Tl) detector. Then, the FEPE for any source-to-detector distance and incident photon energy is simply calculated based on Eq. (1). The uncertainty of calculated FEPE is determined by the propagation error formula with the uncertainty components of h_0, the position of radioactive point source and the FEPE at reference distance x_0. The reliability of the VPD model for the FEPE calculation is evaluated based on the relative deviation of calculated and experimental results. The relative deviation (RD) is determined by the following equation detectors (Osvath et al., 2016; Chuong et al., 2019):

$$RD(\%) = \frac{|\varepsilon_{Exp} - \varepsilon_{Cal}|}{\varepsilon_{Exp}} \times 100\% \quad (3)$$

where ε_{Exp} and ε_{Cal} are the FEPE of detector obtained from experiment and calculation with VPD model, respectively.

The experimental absolute FEPE is determined by the following equation (Thanh et al., 2018; He et al., 2018):

$$\varepsilon_{Exp}(E) = \frac{N(E)}{A \times I(E) \times t} \times C_{Coin} \times C_{decay} \quad (4)$$

where: N is the net peak area for each energy; A is the source activity (Bq); I is the photon emission probability; t is the acquisition live time (s); C_{decay} is the decay correction factor for the decline of source activity over time; C_{Coin} is the coincidence summing correction factor (CSF) for the complex decay-scheme radionuclides. The coincidence summing effect is significant for source-to-detector close geometries and thus it cannot be neglected for determining experimental FEPE. In this study, the calculation of CSF for NaI(Tl) detectors has been performed using the MCNP-CP code (Andrey, 2006). The reliability of the MCNP-CP code for the calculation of CSF has been confirmed in the previous studies (Thanh et al., 2018; Zhu et al., 2008).

3. Experimental set-up

Two NaI(Tl) detectors of model 802 supplied by Mirion Technologies Inc., 2017a, which have nominal scintillation crystal dimensions of 5.08 × 5.08 cm (detector-A) and 7.62 × 7.62 cm (detector-B), are used in this study (see Fig. 2). The NaI(Tl) detectors are connected to Osprey™ modules (Mirion Technologies Inc., 2017b) based on advanced digital signal processing techniques, ensuring high-voltage supply, amplification, and shaping of the output pulses. The Osprey™ module is linked through the USB connector to the control and data acquisition system. The acquisitions of gamma-ray spectra are driven by Genie-2k version 3.3 software. All spectra are recorded using over 2048 channels. To reduce the channel shifting of NaI(Tl) detectors (Moghaddam et al., 2006), the spectrometers are set-up in a room with stable environmental conditions (approximate temperature of 26 °C and humidity of 45%). Under such measurement conditions, it is validated that there was no significant channel shift after checking different spectra.

The standard radioactive sources of type D configuration supplied by Eckert & Ziegler Group, including ^{22}Na, ^{60}Co, ^{137}Cs, ^{152}Eu, ^{241}Am with relative uncertainties of the reference activities around 3%, are used to provide gamma-rays with energies in the range of 60–1408 keV. These radioactive sources are disk-shaped made of high strength plastic with a diameter of 25.4 mm and a thickness of 6.35 mm (Eckert & Ziegler). The active diameter of the source is 5 mm, and the window thickness is 2.77 mm. Table 1 summarizes the relevant data for these sources.

The FEPE of detector A and detector B are measured for the radioactive sources located on the symmetry axis of detectors at various source-to-detector distances in the range of 2–40 cm. Specifically, each NaI(Tl) detector is arranged on a support so that the symmetry axis of the detector is parallel to the floor and at a distance of 40 cm from the floor. It helps to reduce the influence of scattering events with the surrounding materials. The radioactive source is placed on a thin plastic sheet that is fixed to a computer numerical control (CNC) scanning system. Based on this CNC scanning system, the radioactive source can be moved to different positions on the symmetry axis of the detector with an uncertainty of 0.01 mm. Therefore, the measurements are precisely set-up to obtain accurate FEPE for different source-to-detector distances. The counting time for each measured spectra is adjusted to obtain the net area in the interesting full energy peaks ranging from 2×10^5 to 2×10^6. The dead-time for most measurements are less than 5%. However, the analyzer automatically corrects dead-time losses because the MCA works in the live-time mode. Besides, the measurement of environmental background radiations also is carried out. For the data analysis, the background spectrum is subtracted from the spectra

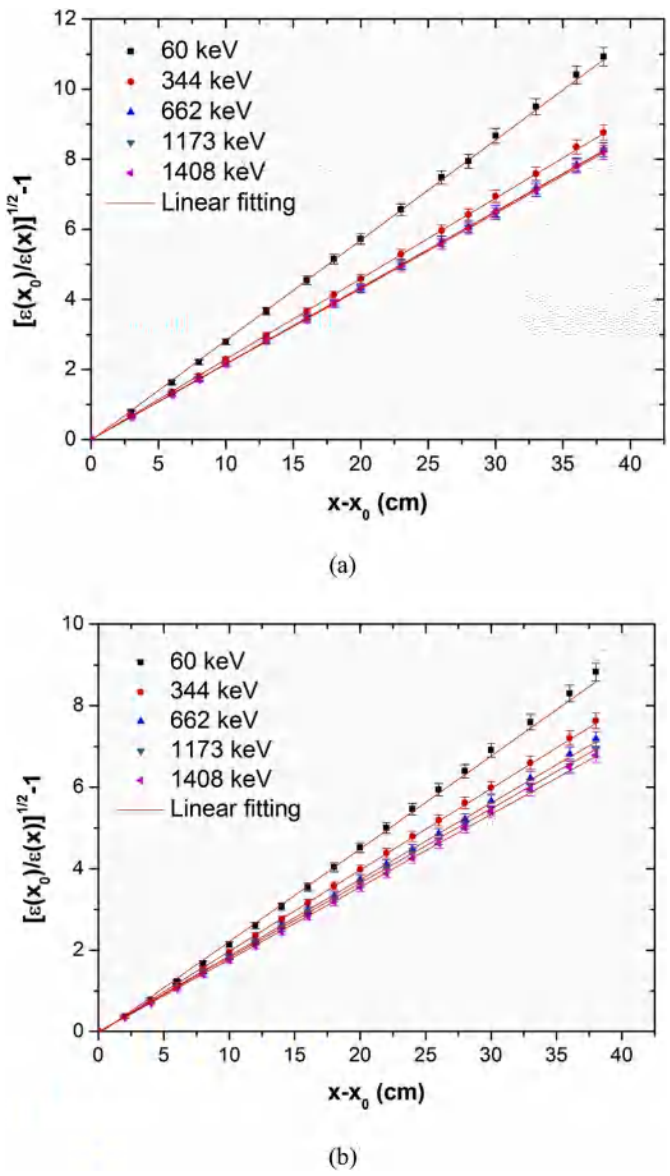

Fig. 3. Linear fitting to experimental data of $\sqrt{\varepsilon(x_0)/\varepsilon(x)} - 1$ versus $(x - x_0)$ for some selected photon energies with (a) detector A and (b) detector B.

obtained with the radioactive sources. Then, these spectra are processed with the COLEGRAM software (Lépy, 2004) that uses the least-squares method to fit mathematical functions to experimental data. The full energy peaks are fitted to a Gaussian function to obtain the net area. The background is fitted by the one-step function or the polynomial function in COLEGRAM software. The choice of an appropriate function for the background depends on the experience of the analyst for the data area of interest. For example, the background is fitted by a one-step function for the 662 keV peak of the ^{137}Cs radioactive source or the fourth-degree polynomial function for the 122 keV peak of the ^{152}Eu radioactive source. However, it must be emphasized that the spectrum processing procedure is the same for all spectra measured from a radioactive source.

4. Results and discussions

4.1. Coincidence summing correction factor

The coincidence summing correction factors of the radioactive sources including ^{22}Na (511, 1274 keV), ^{60}Co (1173, 1332 keV) and ^{152}Eu (122, 344, 779, 964, 1408 keV) for several source-to-detector distances in the range of 2–18 cm for two surveyed NaI(Tl) detectors are presented in Table 2. These CSF values are calculated using the MCNP-CP code with the same geometry as the experiment. The specifications used in the Monte Carlo simulations for detector A and detector B were optimized in our previous studies (Chuong et al., 2019; Sang et al., 2019). The transport of photons in the matter is simulated with the cutoff energy of 1 keV. The F8 tally, which is available in MCNP-CP code, is used to obtain a pulse height spectrum. This is the probability spectrum, which gives the probability for photons to produce an energy-deposit inside in the crystal of the detector at different energy bins. The energy bins in the simulated spectra are set-up based on the energy calibration obtained from the experiments. The method for calculating the CSF value is described in our previous study (Thanh et al., 2018). Monte Carlo simulations are performed with 2×10^9 particles emitting from the source in order to attain good statistics. Thus, the relative uncertainties of the CSF values are less than 1% for all cases. As seen from Table 2, the CSF values are quite high for the source-to-detector distances less than 8 cm, especially for detector B. Obviously, the coincidence summing effect needs to be considered to achieve the accurate experimental FEPE for the source-to-detector close geometries. As the source-to-detector distance increases, the CSF approaches the value of 1. For the source-to-detector distances greater than 18 cm, the coincidence summing effect is insignificant for two surveyed NaI(Tl) detectors and therefore it is not necessary to correct for these geometries.

4.2. Validation of VPD model for NaI(Tl) detectors

Fig. 3 displays the linear fitting to experimental data of $\sqrt{\varepsilon(x_0)/\varepsilon(x)} - 1$ versus $(x - x_0)$ for two surveyed NaI(Tl) detectors for some selected photon energies with reference distance $x_0 = 2$ cm. It can be observed that there is a good agreement between the experimental points and the linear fitting functions. Table 3 shows that the values of the correlation coefficients R^2 and the intercept coefficients are very close to 1 and 0 in all cases, respectively. The same results are also obtained for the reference distances of 10, 20, 30, 40 cm. The correlation coefficients R^2 of the linear fitting functions are unchanged for the different reference distances (for example $x_0 = 2$ cm and $x_0 = 30$ cm as shown in columns 4 and 7 of Table 3). These results confirm the validity of the VPD model for the NaI(Tl) detectors in the surveyed source-to-detector distances and incident photon energies.

In a more detailed evaluation, the differences of the correlation coefficients R^2 from 1 and the intercept coefficients from 0 for the photon energies of 60 and 122 keV are greater than the remaining photon energies. These differences are presented more clearly for the detector B. It shows that the application of a linear function to fit experimental data for low photon energies (60 and 122 keV) is not as good as the photon energies higher than 344 keV, especially with the large dimensions detectors. These results can be explained by the absorption of incident photons in the end cap and the reflector of NaI(Tl) detectors. Specifically, the length (denoted by l) of the moving path of incident photons in the end cap or the reflector is calculated as follows $l = d\sqrt{1 + tg^2(\theta)}$. Where d is the thickness of the end cap or the reflector, θ is the angle created by the directions of the incident photons and the symmetry axis of the detector. For the source-to-detector far geometries, the values of l are almost approximated by d, because the values of θ are very small for all incident photons. However, for the source-to-detector close geometries, the values of l can be much larger than d, because the values of θ can be very large for the incident photons which are directed to the positions located far from the center of the detector. It causes the absorption of the incident photons in the end cap and the reflector for the close geometries to be larger than the far geometries. This effect affects the variation of the FEPE according to the source-to-detector distance. In particular, this effect is significant for low photon energies, but it can be

Table 3
Values of slope, intercept and correlation coefficients R^2 for two surveyed NaI(Tl) detectors for photon energies in the range of 60–1408 keV, with $x_0 = 2$ cm and $x_0 = 30$ cm.

Energy (keV)	$x_0 = 2$ cm			$x_0 = 30$ cm		
	Slope (cm^{-1})	Intercept (cm)	R^2	Slope (cm^{-1})	Intercept (cm)	R^2
NaI(Tl) 5.08 × 5.08 cm detector (Detector A)						
60	0.2858 (15)	−0.0266 (125)	0.9996	0.0320 (2)	0.0037 (42)	0.9996
122	0.2759 (18)	−0.0324 (151)	0.9994	0.0315 (2)	−0.0079 (51)	0.9994
344	0.2298 (4)	−0.0065 (38)	1.0000	0.0310 (1)	0.0011 (14)	1.0000
511	0.2200 (1)	−0.0006 (7)	1.0000	0.0307 (1)	−0.0008 (3)	1.0000
662	0.2171 (2)	−0.0038 (19)	1.0000	0.0307 (1)	0.0011 (7)	1.0000
779	0.2160 (4)	−0.0073 (40)	0.9999	0.0306 (1)	−0.0016 (14)	0.9999
964	0.2188 (5)	−0.0043 (45)	0.9999	0.0307 (1)	−0.0002 (16)	0.9999
1173	0.2165 (3)	0.0032 (33)	1.0000	0.0307 (1)	0.0011 (12)	1.0000
1275	0.2139 (2)	0.0002 (23)	1.0000	0.0307 (1)	0.0040 (8)	1.0000
1333	0.2143 (3)	0.0008 (26)	1.0000	0.0306 (1)	0.0008 (9)	1.0000
1408	0.2153 (3)	−0.0011 (32)	1.0000	0.0307 (1)	0.0010 (12)	1.0000
NaI(Tl) 7.62 × 7.62 cm detector (Detector B)						
60	0.2275 (22)	−0.0626 (190)	0.9984	0.0308 (3)	−0.0120 (70)	0.9984
122	0.2298 (23)	−0.0631 (202)	0.9982	0.0305 (3)	−0.0221 (74)	0.9982
344	0.1996 (7)	−0.0223 (67)	0.9998	0.0302 (1)	−0.0075 (25)	0.9998
511	0.1882 (4)	−0.0134 (41)	0.9999	0.0301 (1)	−0.0011 (16)	0.9999
662	0.1874 (4)	−0.0095 (41)	0.9999	0.0302 (1)	0.0035 (16)	0.9999
779	0.1829 (6)	−0.0115 (55)	0.9998	0.0300 (1)	0.0034 (21)	0.9998
964	0.1848 (4)	−0.0028 (38)	0.9999	0.0297 (1)	−0.0069 (15)	0.9999
1173	0.1825 (2)	−0.0007 (21)	1.0000	0.0299 (1)	0.0002 (8)	1.0000
1275	0.1810 (3)	−0.0055 (34)	0.9999	0.0297 (1)	−0.0045 (13)	0.9999
1333	0.1804 (2)	0.0012 (22)	1.0000	0.0298 (1)	0.0003 (8)	1.0000
1408	0.1781 (5)	−0.0087 (49)	0.9999	0.0297 (1)	−0.0045 (19)	0.9999

negligible for sufficient high photon energies.

4.3. The determination of the VPD position (h_0)

The values of h_0 and associated uncertainties for different photon energies in the range of 60–1408 keV for the two surveyed NaI(Tl) detectors (with $x_0 = 2$, 10, 20, 30, 40 cm) are presented in Table 4. It can be seen that the values of h_0 at the same energy for detector B are larger than those for detector A in all cases. This result is explained by the difference in the crystal dimensions of these Na(Tl) detectors. Rubin et al. (2019) reported the dependence of h_0 on the NaI(Tl) crystal dimensions based on Monte Carlo simulation data. In the case of crystal length equals to its diameter, the value of h_0 increases with the increasing of crystal dimensions.

Besides, the variations of h_0 versus the incident photon energy for the two surveyed NaI(Tl) detectors are also shown in Fig. 4. Although that the values of h_0 at an energy of 60 keV are larger than the ones at an energy of 122 keV in some cases with different reference distances, and there are a few quite large fluctuations of experimental points. But, in general, the value of h_0 increases with the increasing of incident photon

Table 4
Values of h_0 and associated uncertainties for different photon energies for the two surveyed NaI(Tl) detectors with different reference distances $x_0 = 2$, 10, 20, 30, 40 cm.

Energy (keV)	h_0 (cm)				
	$x_0 = 2$ cm	$x_0 = 10$ cm	$x_0 = 20$ cm	$x_0 = 30$ cm	$x_0 = 40$ cm
NaI(Tl) 5.08 × 5.08 cm detector (Detector A)					
60	1.222 (19)	0.960 (60)	1.224 (115)	1.012 (167)	1.459 (222)
122	1.348 (24)	0.974 (74)	1.187 (141)	1.479 (208)	1.811 (276)
344	2.074 (8)	1.973 (22)	2.020 (40)	2.012 (58)	2.204 (77)
511	2.268 (2)	2.265 (4)	2.266 (8)	2.286 (11)	2.294 (14)
662	2.329 (4)	2.280 (12)	2.256 (21)	2.275 (30)	2.422 (40)
779	2.352 (9)	2.250 (24)	2.291 (44)	2.371 (63)	2.403 (83)
964	2.293 (10)	2.165 (27)	2.139 (48)	2.275 (70)	2.422 (92)
1173	2.342 (8)	2.413 (21)	2.373 (37)	2.318 (53)	2.513 (69)
1275	2.398 (5)	2.420 (14)	2.419 (25)	2.264 (36)	2.550 (48)
1333	2.390 (6)	2.446 (16)	2.455 (29)	2.371 (41)	2.385 (54)
1408	2.368 (7)	2.276 (20)	2.388 (36)	2.328 (51)	2.422 (67)
NaI(Tl) 7.62 × 7.62 cm detector (Detector B)					
60	2.118 (42)	1.484 (111)	1.852 (209)	2.233 (307)	2.920 (408)
122	2.075 (44)	1.394 (117)	1.847 (221)	2.521 (328)	2.994 (433)
344	2.733 (18)	2.485 (45)	2.643 (81)	2.869 (117)	2.976 (153)
511	3.038 (12)	2.874 (29)	2.968 (52)	3.001 (74)	3.239 (97)
662	3.059 (12)	2.951 (29)	2.882 (51)	2.890 (73)	3.410 (96)
779	3.191 (17)	3.121 (41)	2.973 (71)	3.012 (101)	3.353 (132)
964	3.135 (11)	3.155 (28)	3.181 (49)	3.348 (71)	3.391 (92)
1173	3.204 (6)	3.237 (15)	3.203 (27)	3.190 (38)	3.220 (50)
1275	3.247 (10)	3.149 (25)	3.186 (44)	3.370 (63)	3.506 (82)
1333	3.265 (7)	3.301 (17)	3.325 (29)	3.258 (41)	3.334 (53)
1408	3.338 (15)	3.187 (37)	3.208 (64)	3.438 (92)	3.448 (120)

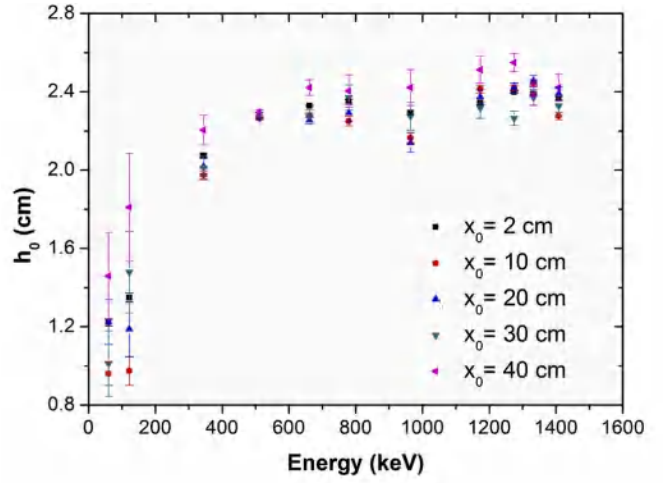

(a)

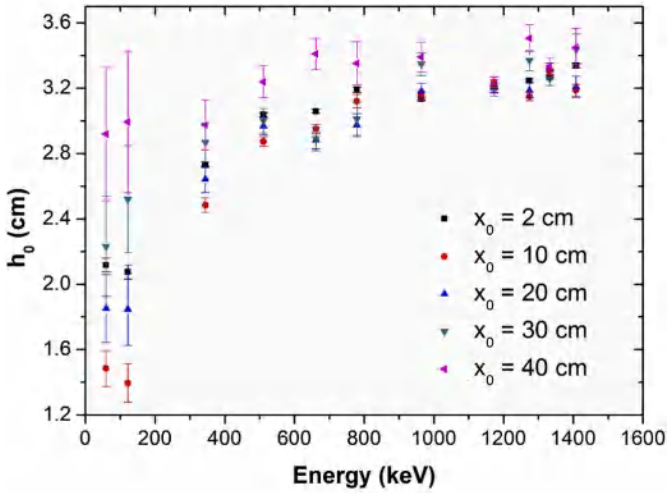

(b)

Fig. 4. Dependence of h_0 on incident photon energy for (a) detector A and (b) detector B with different reference distances x_0 = 2, 10, 20, 30, 40 cm.

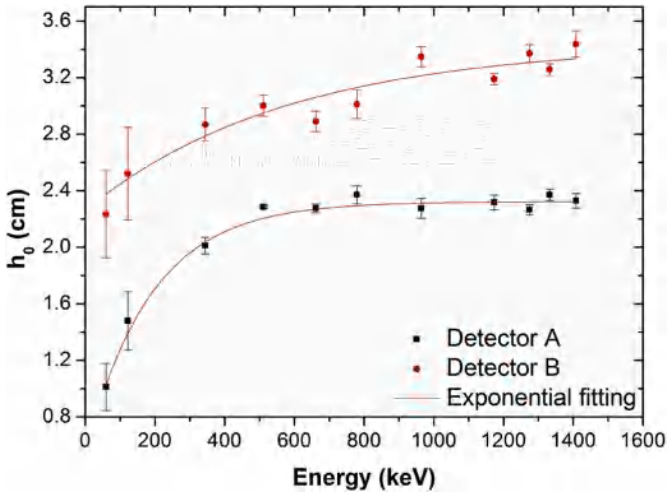

Fig. 5. Exponential fitting to experimental data of h_0 versus incident photon energy for two surveyed NaI(Tl) detectors with reference distance $x_0 = 30$ cm.

energy in the range of 60–511 keV and is approximately the constant for the photon energies higher than 511 keV. The constant value of h_0 is approximately half of the crystal length. This is similar to the behavior observed from Monte Carlo simulation data in case of crystal length equals to its diameter (Rubin et al., 2019). These results claim the dependence of the VPD position on the incident photon energy for the NaI(Tl) detectors. The values of h_0 versus the incident photon energies can be fitted with an exponential function in the following form:

$$h_0(E) = a + be^{cE} \quad (5)$$

where E is the incident photon energy (keV); a, b, c are coefficients of Eq. (5), their values are obtained by the least-square fitting method. Eq. (5) can be used to calculate the value of h_0 for any incident photon energy in the range of 60–1408 keV. Because the value of h_0 depends on the crystal dimensions as mentioned above, the coefficients of Eq. (5) must be determined for each NaI(Tl) detector. Fig. 5 displays the exponential fitting to experimental data of h_0 versus incident photon energy for two surveyed NaI(Tl) detectors with reference distance $x_0 = 30$ cm. The values of a, b, c coefficients respectively are 2.32 (2), −1.78 (23), −0.005 (1) for detector A and 3.44 (20), −1.18 (32), −0.002 (1) for detector B. Table 5 presents the comparison between experimental values of h_0 and calculated values by Eq. (5) for two surveyed NaI(Tl) detectors with reference distance $x_0 = 30$ cm. The maximum deviations and average deviations between experimental and calculated values are less than 7% and 4% for the two NaI(Tl) detectors. These results show

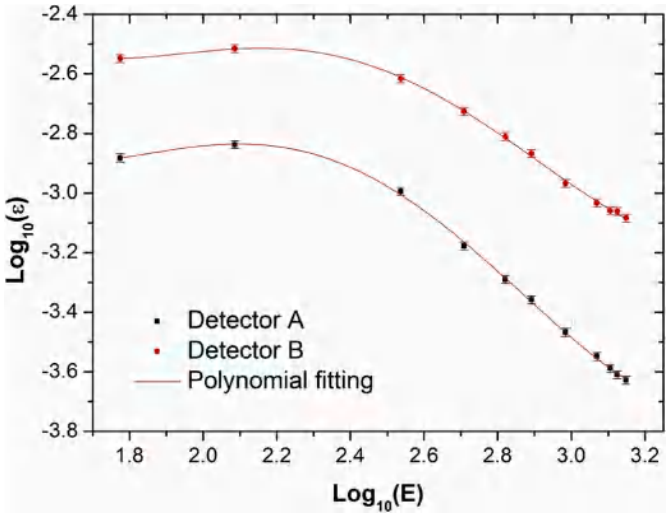

Fig. 6. Polynomial fitting to experimental data of $Log_{10}(\varepsilon)$ versus $Log_{10}(E)$ for two surveyed NaI(Tl) detectors with source-to-detector distance of 30 cm.

Table 6
Values of the relative deviation between experimental and calculated FEPE (by Eq. (8)) at different source-to-detector distances and for detector A.

	Relative deviation (%)							
E (keV)	60	122	344	511	662	779	1173	1408
x (cm)								
2	12.2	2.4	0.8	5.6	3.5	0.4	0.8	2.4
5	2.0	9.8	2.7	4.1	1.4	3.2	0.7	2.3
8	2.7	8.4	3.6	3.7	1.3	2.5	0.4	0.1
10	1.2	7.1	3.5	3.7	1.1	2.8	0.3	0.4
12	0.5	4.8	2.7	3.4	1.4	1.9	0.8	1.4
15	0.2	3.3	2.8	3.3	1.1	0.3	1.0	1.7
18	1.0	3.4	3.2	3.3	1.3	2.8	1.4	0.2
20	1.8	2.0	2.6	3.2	0.8	2.2	1.3	0.9
22	1.8	1.2	2.7	3.3	0.8	2.1	1.3	0.5
25	1.2	0.9	2.2	3.1	1.1	2.3	0.7	0.1
28	2.4	0.3	2.6	3.2	1.5	2.4	3.1	0.1
30	0.1	0.5	2.6	3.2	0.9	1.7	1.7	0.4
32	3.2	2.0	1.1	3.2	1.6	0.6	3.0	1.6
35	2.3	1.5	2.2	2.5	1.5	1.7	2.4	0.7
38	3.1	3.2	0.7	3.2	1.8	1.8	0.9	1.6
40	2.0	1.9	1.7	3.1	1.6	1.7	0.9	0.8
Average	2.4	3.3	2.4	3.5	1.4	1.9	1.3	0.9

Table 5
Comparison between experimental values of h_0 and calculated values by Eq. (5) for two surveyed NaI(Tl) detectors with reference distance $x_0 = 30$ cm.

E (keV)	h_0 (cm)					
	Detector A			Detector B		
	Experiment	Calculated	RD (%)	Experiment	Calculated	RD (%)
60	1.012 (167)	1.025 (180)	1.3	2.233 (307)	2.376 (357)	6.4
122	1.479 (208)	1.391 (149)	6.0	2.521 (328)	2.484 (354)	1.5
344	2.012 (58)	2.037 (84)	1.2	2.869 (117)	2.787 (377)	2.8
511	2.286 (11)	2.205 (51)	3.5	3.001 (74)	2.949 (383)	1.7
662	2.275 (30)	2.270 (33)	0.2	2.890 (73)	3.061 (373)	5.9
779	2.371 (63)	2.294 (25)	3.2	3.012 (101)	3.130 (359)	3.9
964	2.275 (70)	2.312 (20)	1.6	3.348 (71)	3.214 (332)	4.0
1173	2.318 (53)	2.319 (19)	0.1	3.190 (38)	3.281 (299)	2.9
1275	2.264 (36)	2.321 (19)	2.5	3.370 (63)	3.307 (284)	1.9
1333	2.371 (41)	2.321 (19)	2.1	3.258 (41)	3.319 (276)	1.9
1408	2.328 (51)	2.322 (19)	0.3	3.438 (92)	3.333 (267)	3.1
Average			2.0			3.3

RD is relative deviation.

Table 7
Values of the relative deviation between experimental and calculated FEPE (by Eq. (8)) at different source-to-detector distances for detector B.

	Relative deviation (%)							
E (keV)	60	122	344	511	662	779	1173	1408
x (cm)								
2	9.9	16.9	1.8	3.2	0.3	0.7	1.3	1.0
4	17.7	21.7	5.1	0.5	1.8	1.1	1.6	1.4
6	17.4	21.7	6.3	1.4	2.2	3.9	0.4	2.4
8	15.3	19.8	5.3	1.4	2.0	3.4	0.3	3.2
10	12.8	16.8	4.2	1.3	1.9	1.7	0.9	3.3
12	10.5	14.4	3.3	0.8	2.1	1.7	0.9	3.0
14	8.4	11.8	2.4	0.6	1.9	2.4	0.2	2.9
16	6.9	9.6	2.1	0.1	1.5	3.1	0.3	2.9
18	5.1	8.0	1.8	0.1	1.0	2.7	1.6	2.0
20	3.7	6.1	0.8	0.0	1.8	2.9	0.9	2.2
22	2.3	5.0	0.4	0.1	0.6	1.2	1.1	2.0
24	1.1	4.1	0.4	0.3	0.8	2.1	0.9	2.4
26	0.8	3.0	0.1	0.9	0.9	2.4	1.3	2.1
28	0.0	1.9	0.0	0.2	0.7	2.1	0.2	1.5
30	0.1	0.3	0.9	0.1	1.3	2.3	1.0	0.5
32	1.6	1.8	0.2	1.7	0.9	0.7	1.3	0.7
35	1.6	0.9	0.5	0.3	0.8	0.8	1.9	0.8
38	2.0	0.2	0.7	0.6	1.3	0.9	0.0	0.9
40	3.5	1.8	1.2	1.2	1.3	0.6	1.3	0.6
Average	6.4	8.7	2.0	0.8	1.3	1.9	0.9	1.9

that the value of h_0 can be determined by Eq. (5) with satisfactory accuracy.

4.4. Semi-empirical equation for FEPE calculation

In this section, a semi-empirical equation is proposed based on the VPD model to calculate the FEPE of NaI(Tl) detectors for source-to-detector distances and incident photon energies in the surveyed range. Eq. (1) can be rewritten in the following way:

$$\varepsilon(x,E) = \varepsilon(x_0,E)\left[\frac{x_0 + h_0(E)}{x + h_0(E)}\right]^2 \quad (6)$$

where $\varepsilon(x,E)$ and $\varepsilon(x_0,E)$ are the FEPE in the point source configuration at source-to-detector distances x and x_0 for incident photon energy E; $h_0(E)$ is mentioned in Eq. (5). The reference distance x_0 greater than 20 cm should be selected so that the coincidence summing effect can be ignored in the determination of FEPE. Besides, the dependence of FEPE on incident photon energy can be expressed by the following equation:

$$Log_{10}(\varepsilon) = \sum_{i=0}^{4} \alpha_i [Log_{10}(E)]^i \quad (7)$$

where ε is measured by the experiments; E is in keV; α_i (i = 0, 1, 2, 3, 4) are the coefficients of Eq. (7), their values are obtained by the least-square fitting method. Fig. 6 displays the fourth-degree polynomial fitting to experimental data of $Log_{10}(\varepsilon)$ versus $Log_{10}(E)$ for two surveyed NaI(Tl) detectors with a source-to-detector distance of 30 cm. The correlation coefficients R^2 of these fitting functions are greater than 0.998. The values of α_0, α_1, α_2, α_3, α_4 coefficients respectively are 11.6 (51), −27.7 (86), 19.3 (54), −5.7 (15), 0.61 (15) for detector A and 12.9 (44), −28.2 (75), 18.8 (47), −5.4 (13), 0.55 (13) for detector B.

From Eq. (5), Eq. (6) and Eq. (7), an equation can be expressed as follows:

$$\varepsilon(x,E) = 10^{\sum_{i=0}^{4} \alpha_i [Log_{10}(E)]^i}\left[\frac{x_0 + a + be^{cE}}{x + a + be^{cE}}\right]^2 \quad (8)$$

with a defined x_0, Eq. (8) includes the variables of the source-to-detector distance x and the incident photon energy E. Obviously, this equation can be used to calculate the FEPE of NaI(Tl) detectors at any source-to-detector distance and incident photon energy. Values of the relative deviation between experimental and calculated FEPE (by Eq. (8)) at different source-to-detector distances and incident photon energies for two surveyed NaI(Tl) detectors are presented in Table 6 and Table 7. The uncertainties of the calculated FEPE by Eq. (8) are lower than 4% in all cases. It is observed that the relative deviation between experimental and calculated FEPE is almost less than 4% for photon energies in the range of 344–1408 keV. However, the calculated FEPE show significant discrepancies from experimental FEPE for source-to-detector close geometries for photon energies of 60 and 122 keV. The maximum deviation between experimental and calculated FEPE is up to about 12% for detector A and 22% for detector B. These differences can be explained as discussed in section 4.2.

5. Conclusions

In this study, the validity of the VPD model is confirmed for two surveyed NaI(Tl) detectors (with different crystal dimensions) for incident photon energy in the range of 60–1408 keV. It is verified that the VPD model is valid to fit too well to the experimental data for the whole range from 2 to 40 cm of source-to-detector distance. The dependence of the VPD position on the incident photon energy and the scintillation crystal dimensions is also shown based on experimental data. These results provide a revision of the VPD model for NaI(Tl) scintillation detectors from a previous publication (Presler et al., 2006). Besides, a semi-empirical equation is proposed based on the VPD model to calculate the FEPE for any source-to-detector distance and incident photon energy. The calculated FEPE of two surveyed NaI(Tl) detectors are in a good agreement with experimental FEPE for incident photon energies in the range of 344–1408 keV. However, the difference between experimental and calculated FEPE is quite significant for source-to-detector close geometries and photon energies lower than 344 keV.

Author contribution statement

Huynh Dinh Chuong, Le Thi Ngoc Trang, Vo Hoang Nguyen, and Tran Thien Thanh have contributed in conducting experiments and getting hold of data. Huynh Dinh Chuong, and Tran Thien Thanh have contributed significantly explanation of data and writing the manuscript.

Declaration of competing interest

The authors declare that they have no conflicts of interest.

Acknowledgements

This research is funded by Vietnam National Foundation for Science and Technology Development (NAFOSTED) under grant number 103.04-2017.303.

Appendix A. Supplementary data

Supplementary data to this article can be found online at https://doi.org/10.1016/j.apradiso.2020.109179.

References

Eckert & Ziegler. Catalogue of reference and calibration sources. https://www.ezag.com/fileadmin/user_upload/isotopes/isotopes/Isotrak/isotrak-pdf/Product_literature/EZIPL/EZIP_catalogue_reference_and_calibration_sources.pdf. Accessed 30 July 2019.

Andrey, N.B., 2006. MCNP-CP: a correlated particle radiation source extension of a general purpose Monte Carlo N-particle transport code. Appl. Model. Comput. Nucl. Sci. 13, 183–194.

Chuong, H.D., Hung, N.Q., Le, N.T.M., Nguyen, V.H., Thanh, T.T., 2019. Validation of gamma scanning method for optimizing NaI(Tl) detector model in Monte Carlo simulation. Appl. Radiat. Isot. 149, 1–8.

He, L.C., Diao, L.J., Sun, B.H., Zhu, L.H., Zhao, J.W., Wang, M., Wang, K., 2018. Summing coincidence correction for γ-ray measurements using the HPGe detector with a low background shielding system. Nucl. Instrum. Methods Phys. Res. 880, 22–27.

Hoover, A.S., 2007. Characterization of the virtual point detector effect for coaxial HPGe detectors using Monte Carlo simulation. Nucl. Instrum. Methods Phys. Res. 572, 839–843.

Laboratoire National Henri Becquerel. http://www.nucleide.org/DDEP_WG/DDEPdata.htm. Accessed 30 July 2019.

Lépy, M.C., 2004. Presentation of the COLEGRAM Software. Note Technique LNHB 04/26.

Mahling, S., Orion, I., Alfassi, Z.B., 2006. The dependence of the virtual point-detector on the HPGe detector dimensions. Nucl. Instrum. Methods Phys. Res. 557, 544–553.

Mirion Technologies Inc, 2017. 802 Scintillation Detectors. https://www.mirion.com/products/802-scintillation-detectors. Accessed 30 July 2019.

Mirion Technologies Inc, 2017. Osprey™ – Universal Digital MCA Tube Base for Scintillation Spectrometry. http://www.mirion.com/products/osprey-universal-digital-mca-Tube-base-for-scintillation-spectrometry. Accessed 30 July 2019.

Moghaddam, Y.R., Motavalli, L.R., Hakimabadi, H.M., 2016. Peak shifted properties of the "low background NaI(Tl) detectors": an experimental study of response function behavior in different temperature and acquisition time. Radiat. Phys. Chem. 126, 62–67.

Mohammadi, M.A., Abdi, M.R., Kamali, M., Mostajaboddavati, M., Zare, M.R., 2011. Evaluation of HPGe detector efficiency for point sources using virtual point detector model. Appl. Radiat. Isot. 69, 521–526.

Notea, A., 1971. The Ge(Li) spectrometer as a point detector. Nucl. Instrum. Methods 91, 513–515.

Osvath, I., Tarjan, S., Pitois, A., Groening, M., Osborn, D., 2016. IAEA's ALMERA network: supporting the quality of environmental radioactivity measurements. Appl. Radiat. Isot. 109, 90–95.

Presler, O., German, U., Pushkarsky, V., Alfassi, Z.B., 2006. Virtual point detector: on the interpolation and extrapolation of scintillation detectors counting efficiencies. Nucl. Instrum. Methods Phys. Res. 565, 704–710.

Rubin, T., Brandys, I., Presler, O., 2019. The dependence of the virtual point detector on the scintillation detector dimensions. Nucl. Instrum. Methods Phys. Res. 929, 34–41.

Sang, T.T., Chuong, H.D., Tam, H.D., 2019. Simple procedure for optimizing model of NaI(Tl) detector using Monte Carlo simulation. J. Radioanal. Nucl. Chem. 322, 1039–1048.

Thanh, T.T., Vuong, L.Q., Ho, P.L., Chuong, H.D., Nguyen, V.H., Tao, C.V., 2018. Validation of an advanced analytical procedure applied to the measurement of environmental radioactivity. J. Environ. Radioact. 184–185, 109–113.

Zhu, H., Venkataraman, R., Menaa, N., Mueller, W., Croft, S., Berlizov, A., 2008. Validation of gamma-ray true coincidence summing effects modeled by the Monte Carlo code MCNP-CP. J. Radioanal. Nucl. Chem. 278, 359–363.